Iraqi Journal of Physics, 2020 *Vol.18, No.44, PP. 85-97*
DOI: 10.20723/ijp.18.44.85-97

Study the performance of pentacene based organic field effect transistor by using monolayer, bilayer and trilayer with different gate insulators

Bushra H. Mohammed and Estabraq T. Abdullah

Department of Physics, College of Science, University of Baghdad, Baghdad, Iraq

E-mail: Bushra.hussain11@hotmail.com, Estabrak_talib@yahoo.com

Abstract

In this paper, Pentacene based-organic field effect transistors (OFETs) by using different layers (monolayer, bilayer and trilayer) for three different gate insulators (ZrO_2, PVA and CYEPL) were studied its current–voltage (I-V) characteristics by using the gradual-channel approximation model. The device exhibits a typical output curve of a field-effect transistor (FET). Source-drain voltage (V_{ds}) was also investigated to study the effects of gate dielectric on electrical performance for OFET. The effect of capacitance semiconductor in performance OFETs was considered. The values of current and transconductance which calculated using MATLAB simulation. It exhibited a value of current increase with increasing source-drain voltage.

Key words
Organic field effect transistor, pentacene, gate dielectric, dielectric constant.

Article info.
Received: Dec. 2019
Accepted: Dec. 2019
Published: Mar. 2020

دراسه اداء البنتاسين-ترانزستور ثنائي المجال العضوي باستخدام طبقات متعددة وبوابات العزل

بشرى حسين محمد و استبرق طالب عبد الله

قسم الفيزياء، كلية العلوم، جامعة بغداد، بغداد، العراق

الخلاصة

تم في هذا البحث دراسه خواص تيار-فولتيه باستخدام نموذج التقريب التدريجي للقناة لبنتاسيين- ترانزستور ثنائي المجال العضوي لطبقات متعدده (احاديه، ثنائيه وثلاثية) و لعوازل بوابات مختلفة (اوكسيد الزركانيوم، بولي فاينيل الكحول و CYEPL). يُظهر منحني الاخراج شكل نموذجي لترانزستور تاثير المجال. كما تحقق من فولتيه مصدر-تصريف لدراسه تاثير عازل البوابة على الاداء الكهربائي للترانزستور تأثير المجال العضوي. أُخِذ بنظر الاعتبار تاثير سعات شبه الموصل في اداء ترانزستور تاثير المجال العضوي. تم حساب التيار والموصليه المنقوله باستخدام محاكاه الماتلاب.

Introduction

In the recent years, electronic devices based on organic semiconductors have been the subject of intense research, such as organic light-emitting diodes (OLEDs), organic photovoltaic cells and organic effect field transistors (OEFTs). Among them organic field effect transistors (OFETs) have gained a high interest and have made a tremendous progress from the viewpoint of electronic performance and reliability [1, 2]. Organic semiconductors are generally divided in two main categories: small molecules and polymers. Regarding the electrically active organic compounds used for OFETs, organic semiconductors represent a large class of solids.

Different physical properties of these materials result in their different performance and process ability [3, 4]. Most of today organic semiconductors exhibits p-type conductivity. Semiconducting active layer and gate dielectric are essential components for OFETs. Pentacene is one of the most widely used in OFET due to its high mobility μ_{FET} with a high molecular-weight polymer dielectric layer can reach 1 $cm^2 V^{-1} s^{-1}$. It consists of five linearly-fused benzene rings [5-7].

However, a bottleneck that limits practical applications of OFETs is the high operating voltage, which increases the power consumption of an organic-based circuit [8, 9]. The typical way to overcome this problem is to employ high-k dielectric materials or reduce the thickness of dielectric layers to enlarge the capacitance per unit area of gate dielectrics (C_i) [10-13]. Recently, on the basis of the optical and electrical merits of metal oxide dielectrics, low-voltage OFETs and derived low-power complementary circuits have been achieved by employing high-k metal oxides as the gate dielectrics, such as HfO_2, Al_2O_3 and ZrO_2 [14].

Among these high-k materials, ZrO_2 has attracted great attention due to its high-ε (25.3), wide band gap (5.8 eV) and high refractive index (2.17), with low voltage and low leakage current. The use of ZrO_2 as a gate dielectric in OFET can reduce the operating voltage to a certain degree, but may not enhance the carrier mobility due to the mismatch of surface properties between the insulator and the organic semiconductor. The surface modification on dielectric layers can decrease the defects of the oxide dielectric [15]. Polymer dielectrics can provide a smooth, low trap density surface and a good match with organic semiconductor, such as poly(vinyl alcohol) (PVA) [16] and Cyanoethylpullulan (CYEPL) [17].

In this work, the electrical performance and the effect of semiconductor capacitance were studied of Pentacene organic field-effect transistors (OFETs) for monolayer, bilayer and trilayers for the gate dielectrics (ZrO_2, PVA and CYEPL) by using the gradual-channel approximation model.

Device structure of horizontal OFET

Fig.1 shows the structure of horizontal OFET with top contact configuration. The gate used in this study was Indium Tin Oxide (ITO) (its work function φ=4.78 eV) and three different gate dielectric material with multilayers (monolayer, bilayer and trilayer) ZrO_2, PVA and CYEPL. The organic semiconductor is Pentacene place with gold electrodes for source and drain.

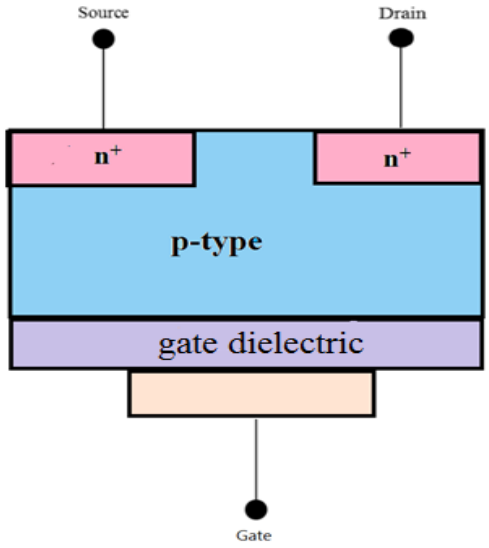

Fig.1: The structure of horizontal organic field -effect transistor (OFET).

Theory

The gradual-channel approximation model can be employed to describe the current flowing across the channel and extract the critical OFET operating parameters. OFETs can be operated in the linear and saturation regions, relying on the quantity of V_d relative to

(V_g-V_{th}). When no V_d is applied to the drain electrode, the positive charge carrier density is uniform across the channel. The application of small V_d, which is less than the efficient gate voltage V_d << (V_g-V_{th}) leads to a linear gradient of charge density within the channel. Hence, the density of mobile charges (Q_{mob}) can be given as [18]:

$$Q_{mob} = n(x)et = C_i\left(V_g - V_{th} - V(x)\right) \quad (1)$$

where C_i is the capacitance per unit area of the gate dielectric, e is the elementary charge ($1.6\text{x}10^{-19}$ C), x is the given position along the channel, t is the thickness of the charged layer in the active channel and $n(x)$ is the number density of charges. This operating regime of OFET-is known as the linear regime. In this regime, the average value of Q_{mob} is $C_i\left(V_g - V_{th} - \frac{V_d}{2}\right)$, which is the areal charge density at the center of the induced channel.

Subsequently, source – drain current:

$$I_d = \frac{WC_i}{L}\mu \times \left[(V_g - V_{th}) \times V_d - \frac{V_d^2}{2}\right] (2)$$

V_d>(V_g-V_{th}) can only push the pinch-off point slightly backward toward the source electrode, and thus yield no extra current. Where the current in the saturation regime:

$$I_d = \frac{WC_i}{2L}\mu_{sat.} \times \left((V_g - V_{th}\right)^2 \quad (3)$$

As the transconductance in linear and the saturation region is given by [19, 20]

$$g_m = \frac{\partial I_D}{\partial V_g} = \mu C_i \frac{W}{L} V_D \quad (4a)$$

the Linear region

$$g_m = \frac{\partial I_D}{\partial V_g} = \mu C_i \frac{W}{L}.\left(V_g - V_{th}\right) \quad (4b)$$

the saturation region.

The MATLAB software was used to calculate the I-V characteristics of this model.

Results and discussion

A. Output characteristics

The (I_d-V_d) characteristics of the pentacene based horizontal OFETs for monolayer, bilayer and trilayer of different gate insulators (ZrO_2, PVA and CYEPL) were presented. These output characteristics have been taken by using the parameters that shown in Tables 1 and 2 which were measured by using Eqs.(2, 3) based on the gradual channel approximation at low drain-to-source voltage.

Table 1: Parameters used [21].

Parameter	Value
length of channel	$4\text{X}10^{-6}$ m
width of channel	$300\text{X}10^{-6}$ m
Mobility	0.15 m/V.s
threshold voltage	-2.5 Volt
Dielectric thickness	$300\text{X}10^{-9}$ m
Semiconductor thickness	$1600\text{X}10^{-9}$ m

Table 2: Dielectric constant for dielectric materials and semiconductor [22, 23].

Dielectric Materials		**Dielectric Constant**
poly(vinyl alcohol)	PVA	7-8
cyanoethylpullulan	CYEPL	10-18
Pentacene		4
zirconium dioxide	ZrO_2	25.3

Figs. 2-7 represent the I_d-V_d for different gate voltages (V_g=-40 to 0 V) of the monolayer, bilayer and trilayer for three different gate insulators (ZrO_2, PVA and CYEPL). These devices showed typical output curves of the horizontal OFET which indicates that only holes are accumulated at the pentacene-dielectric interface, the current flow from the source to the drain through the channel region when negative gate voltages are applied. It can be observed in these curves the increase of V_g leads to increase in the current till reaching its highest value at -40 V for all the different gate insulators. The decrease in the values of current is due to the shift in the threshold voltage by about -2.5 V towards negative voltages. This behaviour is typical for a p-type horizontal OFETs when traps are present at pentacene/insulator interface. Where the output characteristics can be distinguished in respect to the linear, the pinch-off and the saturation regimes which indicates a good ohmic contact pentacene and contact electrodes (Au).

Table 3 shows the highest current can be obtained for different gate insulators (ZrO_2, PVA and CYEPL) in OFETs at V_g= -40 V. An improvement of the drain current can be observed when using ZrO_2 insulator against (PVA and CYEPL) insulators in monolayer, such behavior can be attributed to the increase of effective capacitance (C_i= 7.4635x10^{-4} nF) since ZrO_2 has high dielectric constant (ε =25.3), (as shown in Fig.3, which is defined as [24]:

$$C_i = \varepsilon_\circ \varepsilon / t \quad (5)$$

The carrier charge density is also high according to Eq.(6):

$$Q = C_i(V_g - V_T) \quad (6)$$

This result agrees with many previous works and what is reported by ITRS (International Technology Roadmap for Semiconductors) when using materials with high - dielectric constant [25-29].

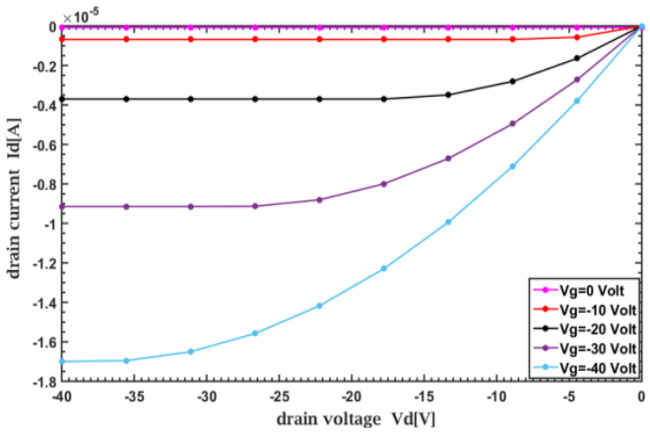

Fig.2: Output characteristic of gate insulator ZrO_2 of the pentacene based horizontal OFET.

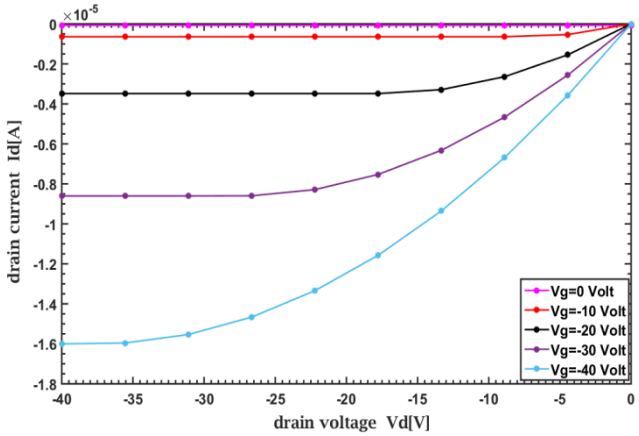

Fig.3: Output characteristic of gate insulator PVA of the pentacene based horizontal OFET.

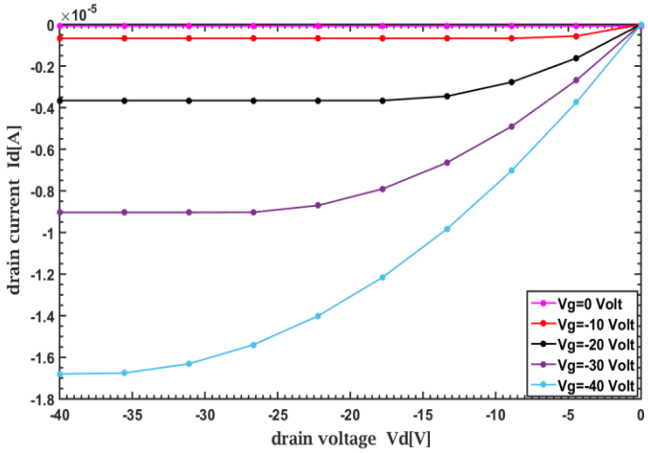

Fig.4: Output characteristic of gate insulator CYEPL of the pentacene based horizontal OFET.

For bilayer, the high values of the drain current can be observed for two dielectric materials (ZrO_2/CYEP), as illustrated in Fig.6. These high values of the drain current can be associated with the high capacitance of the (ZrO_2/CYEPL) layer, which is shown in by the equation [30, 31]:

$$1/C_{total} = 1/C_{Oxide} + 1/C_{polymer} \quad (7)$$

These results are in good agreement with the results of Yea et al. [32].

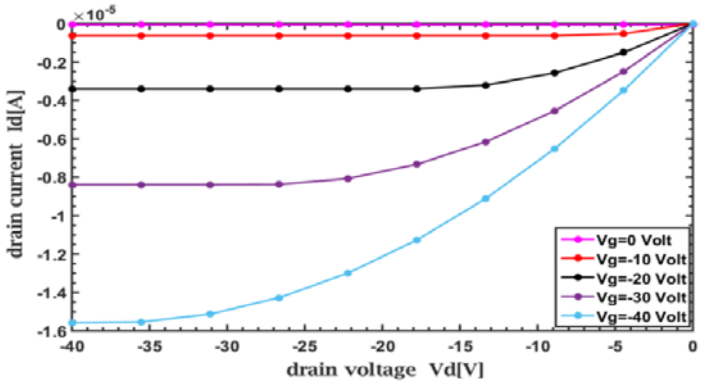

Fig.5: Output characteristic of two gate insulators ZrO_2/ PVA of the pentacene based horizontal OFET.

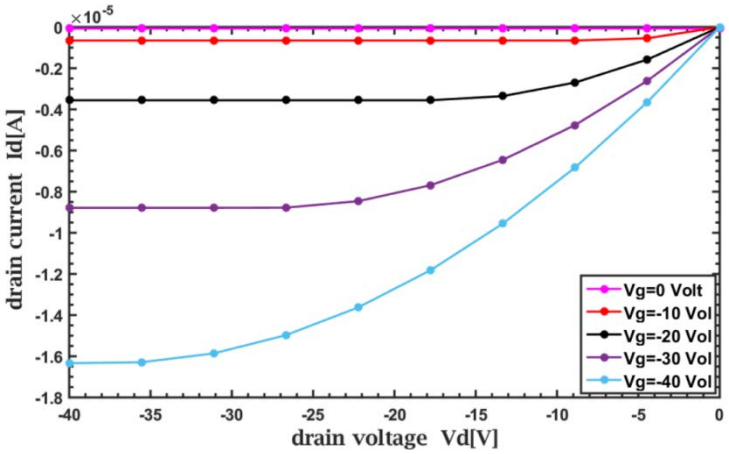

Fig.6: Output characteristic of two gate insulators ZrO_2/ CYEPL of the pentacene based horizontal OFET.

For further improvement, the performance of OFETs with trilayers of different gate insulators (ZrO_2/PVA/CYEPL) were used shown in Fig.7.

The best drain current value was for (ZrO_2/ PVA/ CYEPL). This can be associated with the high capacitance of these three gate insulators, according to the relations [33]:

$1/C_{total} = 1/C_{Oxide} + 1/ C_{polymer1} + 1/C_{polymer2}$

$1/C_{total} = 1/(\varepsilon_{\circ}\varepsilon_{oxide} /t) + 1/(\varepsilon_{\circ}\varepsilon_{polymer1} /t) + 1/(\varepsilon_{\circ}\varepsilon_{polymer2} /t)$ (8)

These results are in good agreement with those of Kni et al. [34].

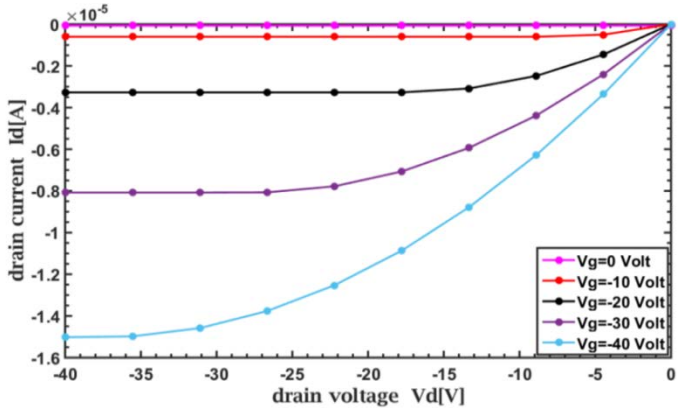

Fig.7: Output characteristic of three gate insulators ZrO_2/ PVA/ CYEPL of the pentacene based horizontal OFET.

Table 3: The highest current for different gate insulators at Vg = -40 V of pentacene horizontal OFET.

Number of layers	Dielectric meterials	$I_{dLinear}$ (A)	$I_{dSat.}$(A)
monolayer	ZrO_2	-1.695×10^{-5}	-1.6997×10^{-5}
	PVA	-1.596×10^{-5}	-1.6001×10^{-5}
	CYEPL	-1.680×10^{-5}	-1.6801×10^{-5}
bilayer	ZrO_2/PVA	-1.554×10^{-5}	-1.5579×10^{-5}
	ZrO_2/CYEPL	1.629×10^{-5}	-1.6336×10^{-5}
trilayer	ZrO_2/PVA /CYEPL	-1.498×10^{-5}	-1.5022×10^{-5}

B. Transfer characteristics

Figs.8-10 show the (I_d-V_g) characteristics of the pentacene based horizontal OFET for the monolayer, bilayers and trilayers of three different gate insulators (ZrO_2, PVA and CYEPL). Transfer characteristics are obtained using Eqs. (2 and 3). transconductance (g_m) are obtained using Eqs. (4a and 4b) based on gradual channel approximation model. The parameters used in Eqs. (2-4), are found in tables 1 and 2.

For theses Figs. 8-19, the same behavior was found, the drain bias increases forcing the drain field to lower the source to channel barrier which increases the charge carrier Q at the beginning of the channel and the charge carrier will cross the barrier, which eventually leads to increase in the drain current.

The best values of the drain current were obtained for monolayer gate insulator (ZrO_2) comparing with the other gate insulators (PVA and CYEPL), Fig.8. This is due to the fact that the gate insulator (ZrO_2) has high dielectric constant, this increases the capacitance, according to the Eq. (1).

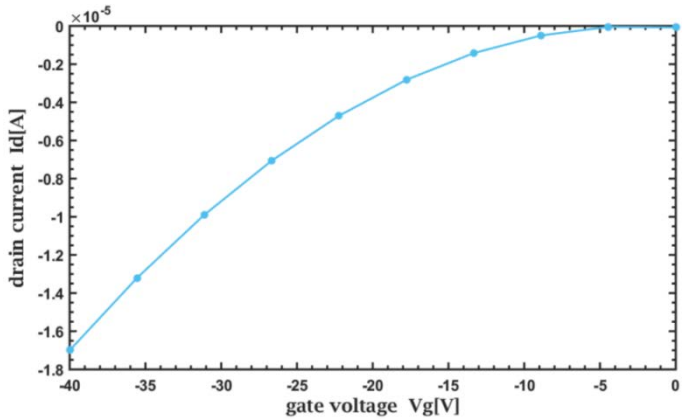

Fig.8: Transfer characteristics at drain voltage -40V of the pentacene based horizontal OFETs of gate insulator (ZrO_2).

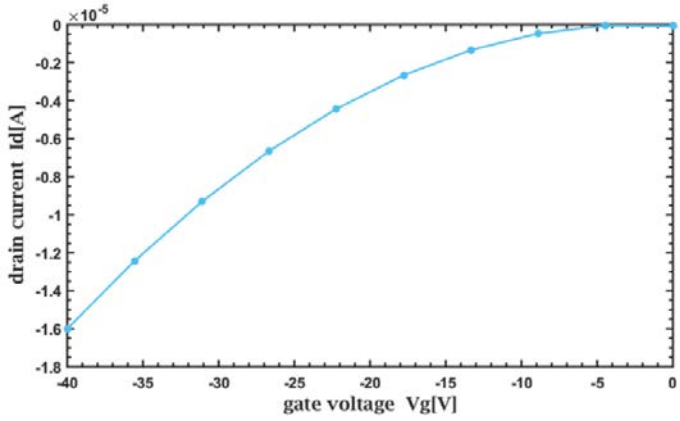

Fig.9: Transfer characteristics at drain voltage -40V of the pentacene based horizontal OFETs of gate insulator (PVA).

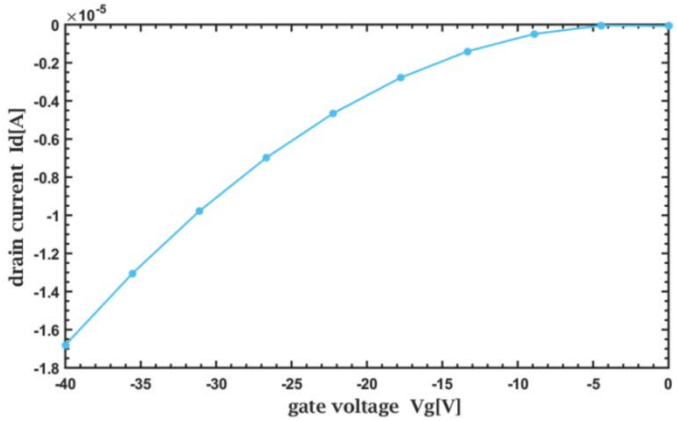

Fig.10: Transfer characteristics at drain voltage -40 V of the pentacene based horizontal OFETs of gate insulator (CYEPL).

In Figs. 11-19, the transconductance was plotted as a function of gate voltage for pentacene horizontal OFET at drain voltage -40 V for different gate insulators (ZrO_2, PVA and CYEPL) and the values were shown in Table 4. It can be noted that the value of transconductance using ZrO_2 as the insulator is better than those for (PVA and CYEPL) (Fig. 11). This behavior is in agreement with Demir et al. [35].

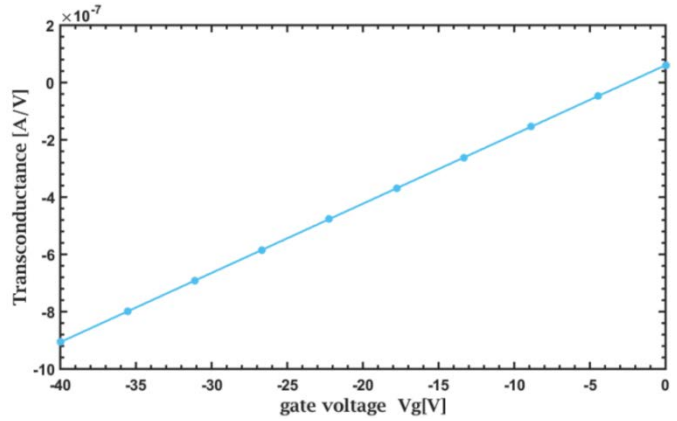

Fig.11: Transconductance at drain voltage -40V for pentacene horizontal OFET of gate insulator (ZrO_2).

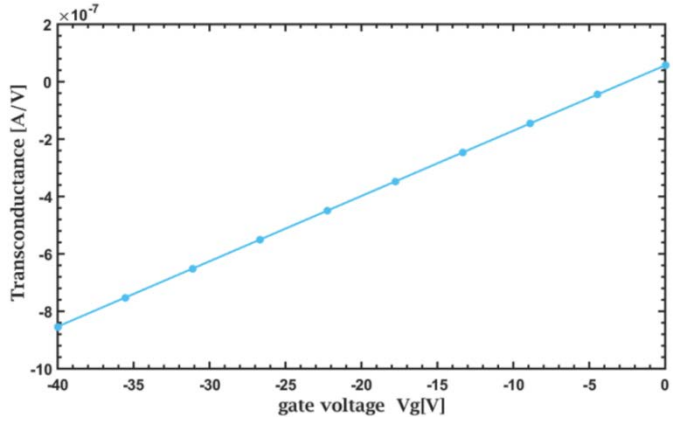

Fig.12: Transconductance at drain voltage -40V for pentacene horizontal OFET of gate insulator (PVA).

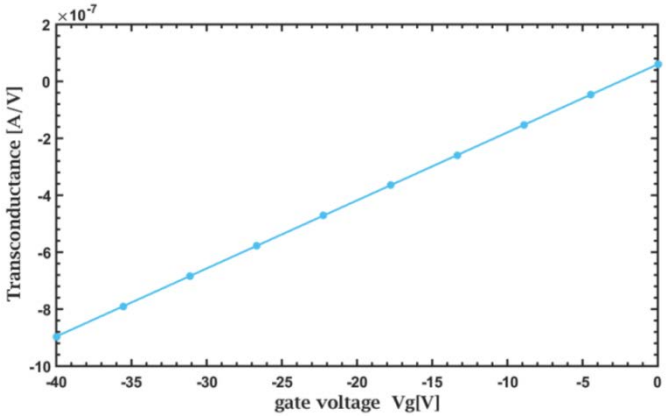

Fig.13: Transconductance at drain voltage -40V for pentacene horizontal OFET of gate insulator (CYEPL).

For bilayer, Figs.14-16, it is clear that as the drain bias increases the drain current increases. This behavior is similar to the behavior of pentacene of horizontal OFET using monolayer of gate insulators.

The decrease of the drain current can be attributed to the threshold voltage shift only. Best results of the drain current were obtained for the two layers of gate insulator (ZrO_2/CYEPL), as illustrated in Fig.15, to this gate insulator (ZrO_2/CYEPL) has high dielectric constant increases the capacitance, according to the relation (7). This result agrees with many previous works and with what is expected by ITRS (International Technology Roadmap for Semiconductors) using material of high - dielectric constant [36].

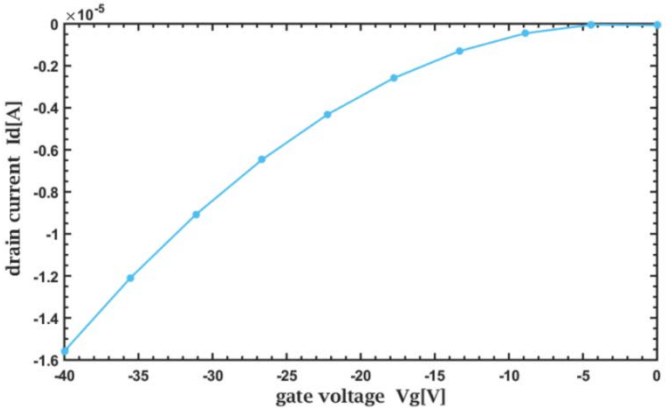

Fig.14: Transfer characteristics at drain voltage -40V of pentacene of horizontal OFET for two layers of gate insulators (ZrO_2/ PVA).

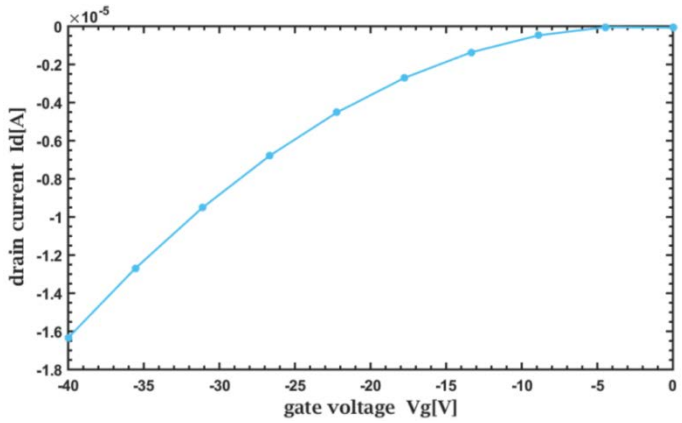

Fig.15: Transfer characteristics at drain voltage -40V of pentacene of horizontal OFET for two layers of gate insulator (ZrO_2/ CYEPL).

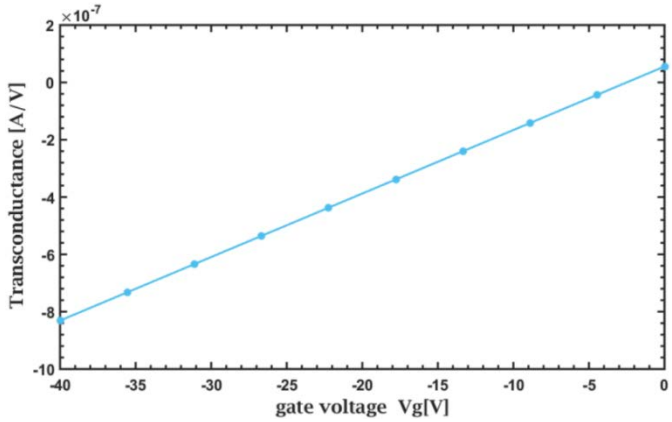

Fig.16: Transconductance at drain voltage -40V of pentacene of horizontal OFET for two layers of gate insulator ZrO_2/PVA.

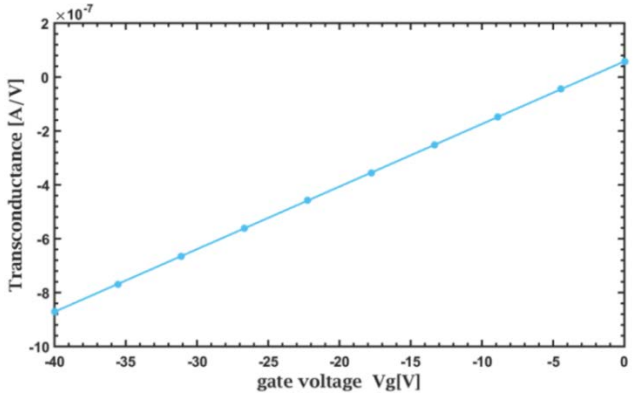

Fig.17: Transconductance at drain voltage -40V of pentacene of horizontal OFET for two layers of gate insulator ZrO_2/CYEPL.

Transconductance for trilayer illustrated in Fig.18-19. Also the decrease in the drain current is caused by the threshold voltage only. This result agrees with many studies and with what is expected by ITRS (International Technology Roadmap for Semiconductors) by using material of high - dielectric constant [33]. The best Transconductance was noticed for (ZrO_2/ PVA/ CYEPL) in Fig.19. This behavior agreement with [35].

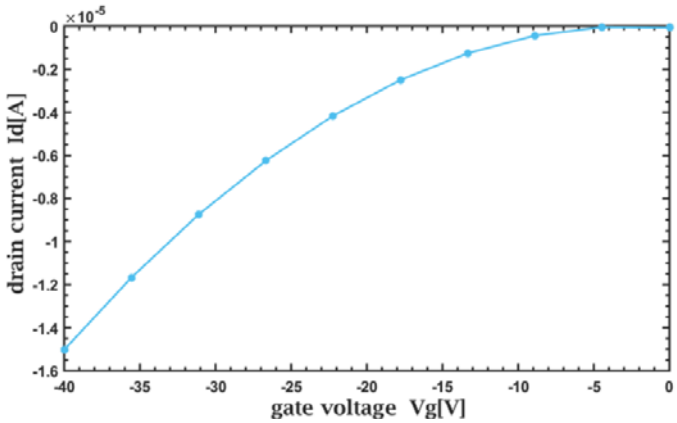

Fig.18: Transfer characteristics at drain voltage -40V of pentacene of horizontal OFET for three layers of gate insulator (ZrO_2/ PVA/ CYEPL).

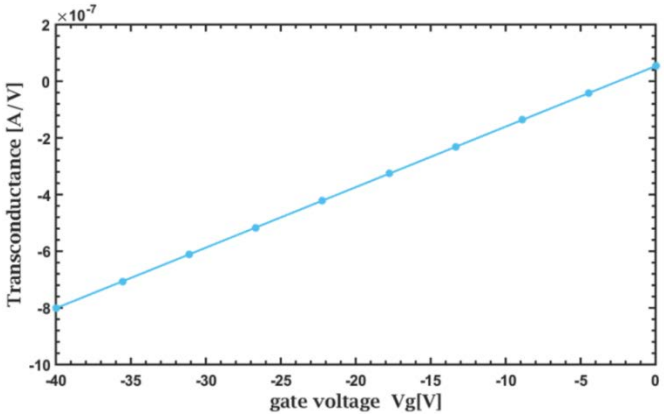

Fig.19: Transconductance at drain voltage -40V of pentacene of horizontal OFET for three layers of gate insulator ZrO_2 /PVA/(CYEPL).

Table 4: The highest value and transconductance for different gate insulators of pentacene horizontal OFETat Vg = -40 Volt.

Number of layers	Dielectric materials	$I_{dlinear}$(A)	$I_{dSat.}$(A)	g_m(A/V)
monolayer	ZrO_2	- 1.692x10^{-5}	- 1.7x10^{-5}	- 0.9065x10^{-6}
	PVA	- 1.593x10^{-5}	-1.6x10^{-5}	- 0.8534x10^{-6}
	CYEPL	- 1.673x10^{-5}	- 1.68x10^{-5}	- 0.8961x10^{-6}
bilayer	ZrO_2/PVA	- 1.554 x 10^{-5}	- 1.5579 x 10^{-5}	- 0.8309 x 10^{-6}
	ZrO_2/CYEPL	-1.629x 10^{-5}	- 1.6336 x 10^{-5}	- 0.8713x 10^{-6}
trilayer	ZrO_2/PVA / CYEPL	- 1.502 x10^{-5}	- 1.502 x10^{-5}	- 0.8012x10^{-6}

Conclusion

OFETs with pentacene as active layers and ZrO_2, PVA and CYEPL as insulating layers were characterized. It is confirmed that the device performance depends on the type of gate insulator and number of layers. The best results of the electrical properties were observed for monolayer of gate insulators compared

with the value of the current for bilayer and trilayer of these gate insulators. Such behavior can be attributed to the effective capacitance.

References

[1] B. Gunduz, Omar A. Al-Hartomy, Said A Farha Al Said, Ahmed A. Al-Ghamdi, F. Yakuphanoglu, Synthetic Metals, 179 (2013) 94-115.

[2] Bahman Kheradmand-Boroujeni, Georg Cornelius Schmidt, Daniel Höft, Reza Shabanpour, Charles Perumal, IEEE Transactions on Electron Devices, 61, 5, May (2014) 1423-1430.

[3] H.T. Yi, M.M. Payne, J.E. Anthony, V. Podzorov, Nat. Commun., 3 (2012) 1259-1265.

[4] Minemawari, T. Yamada, H. Matsui, J. Tsutsumi, S. Haas, R. Chiba, R. Kumai, T. Hasegawa, Nature, 475 (2011) 364-367.

[5] B. Park, Electronic and Structural Properties of Pentacene at Organic / Inorganic Interfaces, University of Wisconsin-Madison, Madison, 2008, Vol 69-05, Section: B, page: 3219, 122 p.

[6] WÖLL, C. Physical and Chemical Aspects of Organic Electronics. Weinheim, Germany: WILEY-VCH Verlag GmbH & Co. KGaA, 2009, page 629,

[7] H. Klauk, M. Halik, U. Zschieschang, G. Schmid, W. Radlik, W. Weber, J. Appl. Phys., 92 (2002) 5259-5263.

[8] T. Hasegawa, J. Takeya, Organic field-effect transistors using single crystals. Sci Tech Adv Mater, 10, 2 (2009) 1-16.

[9] YY. Lin, D.J. Gundlach, S.F. Nelson, TN. Jackson, IEEE Electron Device Lett., 18 (1997) 606-608.

[10] D.J. Gundlach, YY. Lin, T.N. Jackson, S.F. Nelson, D.G.Schlom, IEEE Electron Device Lett., 18 (1997) 87-89.

[11] C.D. Dimitrakopoulos, S. Purushothaman, J. Kymissis, A. Callegari, J.M. Shaw, Science, 283 (1999) 822-824.

[12] Y.M. Park, J. Daniel, M. Heeney, A. Salleo, Adv. Mater., 23 (2011) 971-974.

[13] O. Acton, G. Ting, H. Ma, J.W. Ka, H.-L. Yip, N.M. Tucker, A.K.Y. Jen, Adv. Mater., 20 (2008) 3697-3701.

[14] H. Klauk, U. Zschieschang, J. Pflaum, M. Halik, Nature, 445 (2007) 745- 748.

[15] X. Zhao, S. Wang, A. Li, J. Ouyang, G. Xia, J. Zhou, RSC Adv., 4 (2014) 14890-14892.

[16] Yong Jin Jeong, Dong Hun Kim, Young-Min Kang, Tae Kyu An, Thin Solid Films, 685 (2019) 40-46.

[17] W. He, W. Xu, Q. Peng, C. Liu, G. Zhou, S. Wu, M. Zeng, Z. Zhang, J. Gao, X. Gao, X. Lu, J. M. Liu, J. Phys. Chem., C 120 (2016) 9949-9957.

[18] C. R. Newman, C. D. Frisbie, D. A. da Silva, J. L. Bredas, P. C. Ewbank, K. R. Mann, Chem. Mater., 16 (2004) 4436-4451.

[19] G. Horowitz, J. Mater. Res., 19 (2004) 1946-1962.

[20] D. J. Gundlach, L. Zhou, J. a. Nichols, T. N. Jackson, P. V. Necliudov, M. S. Shur. Journal of Applied Physics, 100, 2 (2006) 024509-1–024509-13.

[21] M.E. Roberts, N. Queralto, S.C.B. Mannsfeld, B.N. Reinecke, W. Knoll, Z. Bao, Chem. Mater., 21 (2009) 2292-2299.

[22] L. Feng, W. Tang, X. Xu, Q. Cui, X. Guo, IEEE Electron Device Lett., 34, 1 (2013) 129-131.

[23] R. Parashkov, E. Becker, G. Ginev, T. Riedl, H.-H. Johannes, and W. Kowalsky, J. Appl. Phys., 95, 3 (2004) 1594-1596.

[24] Yong Xu, Chuan Liu, Dong yoon Khim, Yong-Young Noh, Phys. Chem., 17 (2015) 26545-26552.

[25] Ching-Lin Fan, Ping-Cheng Chiu, and Chang-Chih Lin, IEEE Electron Device Letters, 31, 12, December (2010) 1485-1487.

[26] B. Gunduz, Omar A. Al-Hartomy, Said A Farha Al Said, Ahmed A. Al-Ghamdi, F. Yakuphanoglu, Synthetic Metals, 179 (2013) 94-115.

[27] W. Boukhili, M. Mahdouani, M. Erouel, J. Puigdollers, R. Bourguiga, Synthetic Metals, 199 (2015) 303-309.

[28] Yong Zhang, Caili Lang, Jingze Fan, Lei Shi, Yuanping Yi, Qingjiang Yu, Fengyun Guo, Jinzhong Wang, Liancheng Zhao, Organic Electronics 35 (2016) 53-58.

[29] Qi-Jun Sun, Tan Li, Wei Wu, Shishir Venkatesh, Xin-Hua Zhao, Zong-Xiang Xu, and Vellaisamy A. L. Roy, ACS Applied Electronic Materials, 1, 5 (2019) 711-717.

[30] Xu Yea, Hui Lina, Xinge Yu, Shijiao Hana, Minxia Shanga, Lei Zhanga, Quan Jianga, Jian Zhonga, Synthetic Metals 209 (2015) 337-342.

[31] Hui Lina, Wenqiang Zhaoa, Xiao Konga, Lijuan Lia, Yimeng Lia, Peng Kuanga, Yi Zhanga, Landan Zhanga, Ming Suna, Silu Taoa, Materials Science in Semiconductor Processing, 91 (2019) 275-280.

[32] Yong Jin Jeong, Dong Hun Kim, Young-Min Kang, Tae Kyu, Thin Solid Films, 685 (2019) 40-46.

[33] Georg C. Schmidt, Daniel Hoft, Katherina Haase, Maxi Bellmann, Bahman Kheradmand -Boroujeni, Tomi Hassinen, Henrik Sandberg, Frank Ellinger, Arved C. Hubler1, Polymer Physics, 53 (2015) 1409-1415.

[34] Alessandro Bolognesi, Marco Berliocchi, Maurizio Manenti, Aldo Di Carlo, Member, IEEE, Paolo Lugli, Kamal Lmimouni, Claude Dufour, IEEE Transactions on Electron Device, 51, 12 (2004) 1997- 2003.

[35] Ahmet Demir, Alparslan Atahan, Sadık Bağcı, Metin Aslan, M. Saif Islam, Philosophical Magazine, (2016) 1478-6435.

[36] Abduleziz Ablat, Adrica Kyndiah, Geoffroy Houin, Tugbahan Yilmaz Alic, Lionel Hirsch, Mamatimin Abbas, Scientific Reports, 9, 6685 (2019) 1-8.